Flexibility with Flying:
Replicable and Attachable Aerial Robot with Multi-Degree-of-Freedom

I. Abstract

This project, inspired by the movie Big Hero 6, attempts to create an aerial robot with muti-Degree-of-Freedom (DoF) in the air. Like microbots in Big Hero 6, it aims at creating a drone that could attach to and perform tasks with replicas of itself. Currently, most drones are the market are quadcopter drones with open propellers, losing DoF. This robot, however, created through two ducted fans, could transform shape when attached to replicas of itself. This allows the drone to increase its DoF and flexibility. The drone's mechanical design compost of a thrust rotor module, DoF-Joint Module, two ducted fans, and a Dual-Rotor Gimbal Module. The control uses Kalman Filters and PID, while the practicability of the idea is analyzed through Forward Kinematics (Kinematic Chains and D-H Convention) and classical Force Analysis. These combined, allowed the drone to achieve six DoF in air, with a maximum rotation of 120.73˚ in the x-direction and 114.22˚ in the y-direction, and a constant lift allowing the drone to hover in the air both alone and connected with a replica of itself.

II. Introduction

a. Inspiration

This project was inspired by my all-time favorite movie: Big Hero 6. The idea of microbots, small robots that could transform in shape with almost a six degree of freedom, struck me as genius. The tiny flaw of this setup, however, was when it ran out and failed to push Callaghan into the sky, which resulted in Hiro winning. (YAY!) Despite being super happy when Hiro won, I thought the problem of running out of microbots could be solved if the microbots could fly. If they were able to fly, then Callaghan could simply be carried into the sky, and depending on the scenario, the flying-microbots could change in shape and form. So, my project started with an attempt to solve this problem. with open propellers, and due to this form, they lack in flexibility.

Figure 2.1: A single microbot [20]

Figure 2.2: Microbots Stacked together to form buildings [21]

b. Current Research

Most drones on the market right now are quadcopter drones with open propellers, and due to this form, they lack in flexibility. The goal of this project is to create a drone with 6 degrees of freedom, able of transforming in air, attachable to replicas of itself, and calculate its shape to overcome obstacles that could be in the air, providing flying with flexibility. With the ability to attach to replicas of itself and such flexibility, one drone could be used for multiple purposes. The same drones, for example, could attach to each other for heavy lifting or could detach with each other to scout in multiple directions. Current technology regarding image recognition and forward kinematics allows the drone to recognize images and analyze its position in order to best avoid the images. The main achievement of this project would be to achieve 6 degree of freedom in air and have the mechanical design of a drone to perform tasks in coordination with each other.

Figure 2.2: Current Drones on the market [23]

III. Mechanical Design & Material Selection

a. Thrust Rotor Module

Unlike traditional multi-rotors, this drone needs to achieve 6DoF in air, so rotor disks can't be aligned on the same plane. Currently, there are three ways to achieve such motion: 1) a rotor module controlled by two servos to produce 2DoF tilting 2) a rotor module controlled by a single servo to produce 1DoF tilting, 3) a fixed rotor configuration with different tilt directions.

The first option is applied in this case due to its advantage in accuracy and its ability to make the rotor ground-level. In addition, to support the weight of the rotors and fans, a ridged and lightweight material needs to be used as the main frame; thus, two rod pipes from carbon fiber are adopted. To make

sure the machine could reach the hovering state, symmetry should be attained on both sides. With all these in mind, the basic module is designed.

This module must ensure two axis of rotation around both axis x and axis y. They have the same speed, but in two different directions. The two different directions has two different purposes: both the drag force and the gyroscopic moments would counteract each other. In addition, to ensure rotational inertia, the mass of the entire module has to be as small as possible. Thus, two small rotors with ducted fans is applied for the small mass and high power.

The two rotors are connected to the rods using gears with the following formulas in which:

$$d_o = m(z+2) \tag{1.1}$$

$$d_m = mz \tag{1.2}$$

$$d_i = m(z-2.5) \tag{1.3}$$

$$a = \frac{m(z_1+z_2)}{z} \tag{1.4}$$

$$\frac{n_1}{n_2} = \frac{z_2}{z_1} \tag{1.5}$$

These two gears would be controlled through PID and Karman to ensure that the fans are parallel to the ground.

b. Two DoF-Joint Module

For two drones to connect together, a joint module with two DoF must be implemented. To ensure two DoF movement, two single joint structures are attached together at each end of the drone. Servo A and B move along axis x and y respectively, each with an angle between [-90°, 90°]. This gives two drones connected together a chance to move with 2DoF when needed to complete a specific task. In hovering condition, this connection is expected to serve as a rigid body, providing the stability needed for hovering.

As of currently, two drones could neither attach nor detach automatically. This situation, however, could be improved. Simply by attaching two magnets to both sides of the servo bracket, the assembly of the drones could become automatic. If the drones could hover stable enough to overcome the pulling force applied by these magnets during the assembly, the drone could be controlled to assemble itself in space.

c. Ducted Fans

Ducted fans can be considered to be a hybrid of an open propeller and a turbo engine. There had been a decision between using ducted fans against using propellers. Ducted fans were eventually chosen due to its advantage in speed. With this increase in speed, horizontal lift, resistance, and pitch force would all increase. This allows for greater thrust using the same power as propellers.

Using the an ideal hover case, the following functions could be made:

$$\frac{P_{df}}{P_{op}} = \frac{1}{2\Lambda} \tag{2.1}$$

And the thrust, with the same power, for ducted fans and propellers would be:

$$\frac{T_{df}}{T_p} = \sqrt[3]{2\Lambda} \tag{2.2}$$

In both of these equations, the expansion ratio, $\Lambda = A_e/A$, where A_e is the duct exit area and A is the propeller disk area. From thrust equation, it could bee seen that ducted fans would hold an advantage as long as the expansion ratio is greater than 0.5.

d. CAD Drawing

a. Dual-Rotor Gimbal Module

The position of the two ducted fans were decided to be on the two sides to maintain balance. Two “boxes” would be needed to attach the fan to the carbon fiber rods: one to situate the fan in and another screwed onto the first box would be attaching itself to the rod. The box which the fan

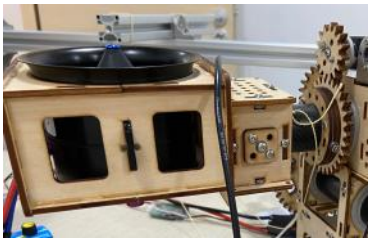

Figure 3.1: Two boxes which attaches the ducted fan to the rod.

Figure 3.2: How the two rods are placed and held in place.

situates in needs to be in two different pieces to be attached to the fan and each of the pieces (the top and bottom of the box) place together to form a hole which locks the fan in place. The second box attached to the first one, as shown in figure has screws on both sides to lock the fan on a fix position on the rod. This prevents the fan from going off the rod in mid flight and allows the fan to turn at the same angle as the rod.

The two rods, which each controls an axis of motion are held in place one on top of the other. The original plan was to drill holes in one of them and let one pass through the other, but was abandoned because it would weaken the strength of the rod. Having the rods held on top of each other would not only strengthen the rod but also allow distance for the gears. Each piece was made also as hollow as possible to eliminate weight of the drone.

b. Servo Attachment

Two pairs of servos are needed on one drone, one pair attaches to the gear sets (which would be called axis servos) and the other pair to attach to other drones (which would be called the attachment servos). The attachment servos are attached onto the rods similar to the way of the fans. They are each attached to a box which is tightened to the rod with a long nail. They are 90

e. Mechanical Material Selection

The drone is made of different parts which could all rotate with regard to each other. Each part has 2DoF, whose rotation would be provided by two servos, one in the x direction and one in the y direction, and the thrust would be provided through the two ducted fans. Each part has a microcontroller attached to it and operate independently controlled by the computer, by signals sent through WIFI. The bird-eye view and the side view are as follows:

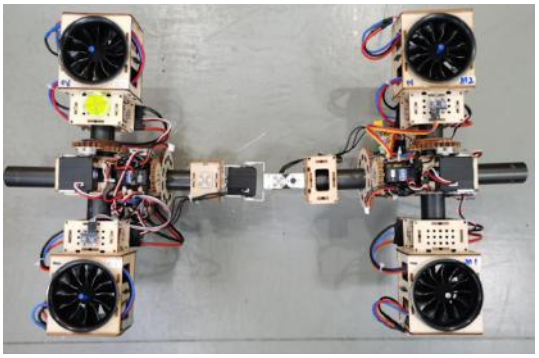

Figure 3.3: The bird-eye view of two drones connected to each other

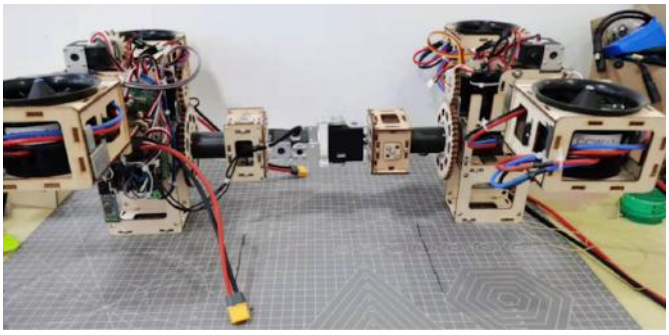

Figure 3.4: The side view of two drones connected to each other

a. Gear

There are two sets of gears that control the x and y direction of rotation. Both of them are activated by independent servos which allows a freedom of rotation from 0° to 300°. The image is as follows:

Figure 3.6: The x-axis gear with respect to the rest of the drone

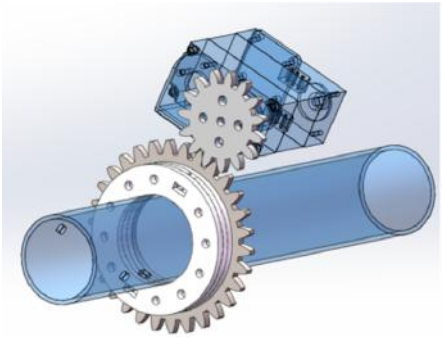

Figure 3.7: Drawing of the x-axis gear on Fusion 360

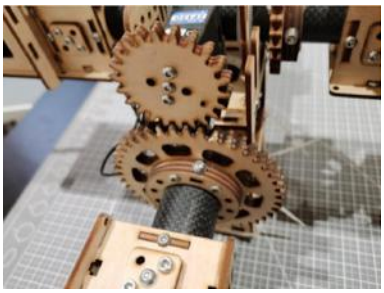

Figure 3.8: The y-axis gear with respect to the rest of the drone

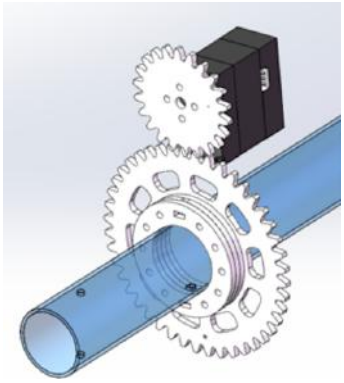

Figure 3.9: Drawing of the y-axis gear on Fusion 360

b. Drone Connection

As shown in the image below, the replicas of the same drone could be connected through a servo, allowing the two drones to achieve rotational motion in both positive and negative direction. This would not only allow the two drones to connect together, but the data from the servo would allow the drone to calculate its position with regard to another.

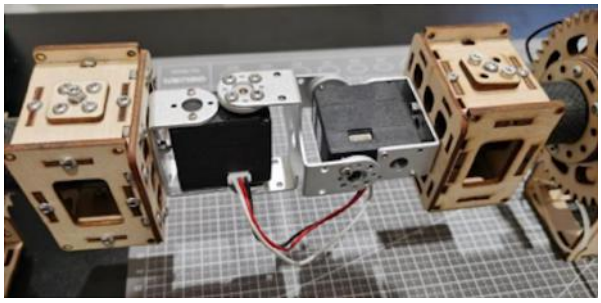

Figure 3.10: The servo connection between two drones

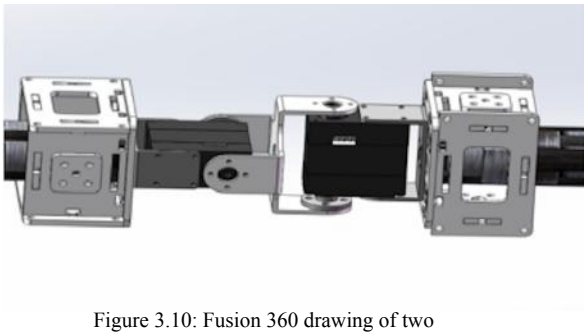

Figure 3.10: Fusion 360 drawing of two drones

c. Attachment of Ducted Fans

The lift of the drone is mainly provided by the ducted fans, which, as shown in the image, is in the middle of the structure together with the gyroscope. To make sure the program runs well with the same angle as programed, the structure has to be parallel.

Figure 3.11: The attachment structure of the fan

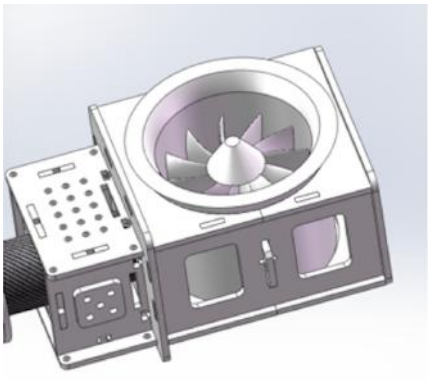

Figure 3.12: Fusion 360 drawing of ducted fan attachment

d. Complete Set

Together, one drone would have a combination of two ducted fans, four servos, two sets of gears, two attachment systems, and two motor units.

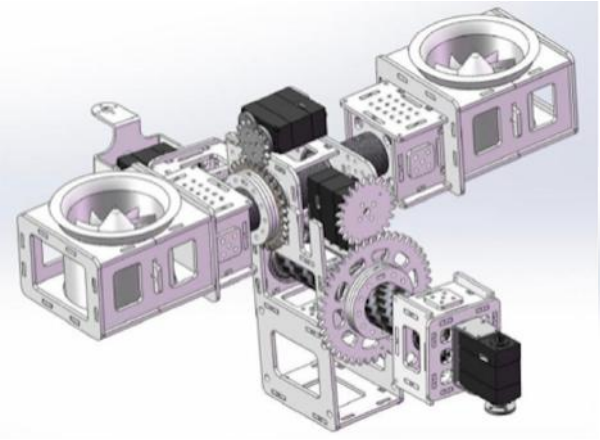

Figure 3.12: A single drone, as drawn on Fusion 360

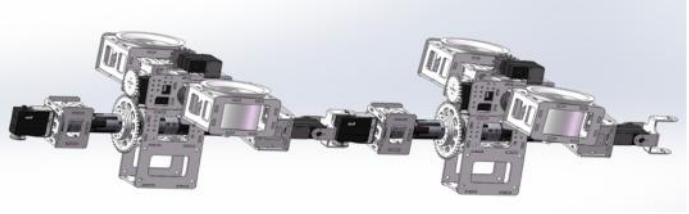

Figure 3.13: Two drones attached together as drawn on Fusion 360

f. Computational Material Selection

a. Microcontroller

The microcontroller used in this drone is called esp32 TTGO, which has a WIFI and bluetooth functions attached, it could achieve wireless communication, and has a 32 bits dual core processor. The CPU oppression speed is 80MHz, with a maximum of 240MHz, the computational ability is as high as 600MIPS. The reason for choosing it was due to its small size and low electric consumption. esp32 is the main controller in the drone and controls the operation of a single unit drone, in which the functions of serial ports, WIFI, IIC, PWM, and more are used. In it serial ports control the servo and transformation of the drone; the WIFI allows each unit drone to be connected and transfer information regarding position; IIC allows the obtaining of gyroscope information; PWM controls the speed of the ducted fans.

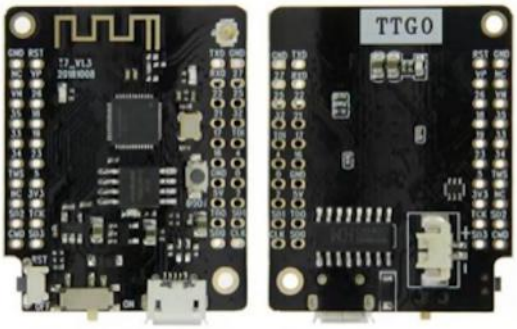

Figure 3.14: esp32 TTGO

b. Servo

Servos on the drone allows the drone both to transform and to be at exact position. An I/O connects the microcontroller with the servo, and the servos are connected to each other through two parts series which allows for less use of serial ports, an easier arrangement of wire, making the project easier, delicate, and simply looks better. Each drone could be arranged an ID number, which allows for recognition. They communicate with each other using signal bus, with a hertz of 115200Hz. Through the ID number the controller could send signals to the different servos, and only servos with the correct ID could receive the signal.

Figure 3.15: Servo

Figure 3.16: Servo Propeller

Figure 3.17: Servo Battery

c. Gyroscope

The gyroscope used in this is MPU650 which obtains the angle and rate of angle change on both the x and y axis; through IIC wire's connection with the microcontroller, the microcontroller obtains the angle and the rate. The processing of the data, in very simple terms, involves elimination of noise through Kalman Filters, which would later be spoke about in the essay.

Figure 3.17: Gyroscope

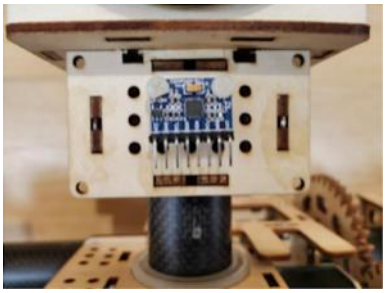

Figure 3.17: Gyroscope on Drone

IV. Movement Dynamics

a. Force Analysis

The force this drone experiences could be separated into two different categories: variable forces and constant forces. Variable forces includes forces such as aerodynamic or aerodynamic torque, and constant forces includes forces such as gravity or air buoyancy. A force diagram of the drone during hovering mode would be something similar to figure 4.1. This part would compose of the analysis for every force dissipated on this diagram and also for forces when the drone is not in hovering mode.

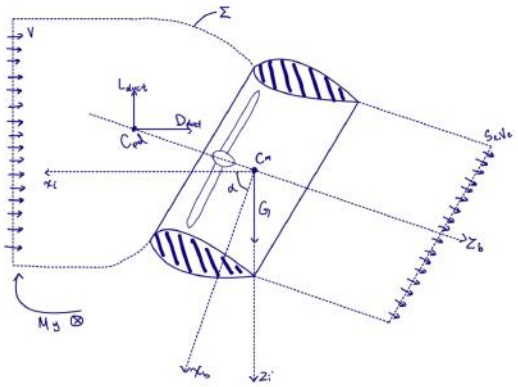

Figure 4.1: Force diagram of drone during hovering.

1. Gravity

Since the drone would mostly be flying near the earth's surface, there wouldn't be a significant change in gravity due to height. Thus, gravity could be modified using this formula:

$$G = mg \tag{3.1}$$

2. Fan Propulsion

From the blade element theory and the momentum theory, the thrust (T) is shown to be related to geometry of the ducted fan and the power (spin speed) of the engine. Here, the equation models T determined on the fluid speed at the out flow for ducted fan (V_e):

$$T = \dot{m}(V_e + V) - \dot{m}V = \rho S_e V_e (V_e + V) \tag{3.2}$$

Where $\dot{m}$ represents the mass flow rate through the duct; V as the relative speed of inflow, and if there aren't any crosswind, it would be the velocity of the drone.

3. Aerodynamic Lift

Regular fixed wing drones's aerodynamic lift could be separated into three parts: wing, hull, and tail aerodynamic lift. The hull's aerodynamic lift is too small, in this drone, to be added to the calculations. The aerodynamic lift and resistance for drones with ducted fans are both dependent on aerodynamic lift and resistance for the ducted fans (L_{duct}) and aerodynamic lift and resistance of the drone's body (L_{CS}). Since this drone doesn't have a body necessary of aerodynamic lift, it will be ignored. Thus the calculations for the lift would be:

$$L = L_{duct} \tag{3.3}$$

Then, due to the symmetrical design of the drone, the zero-lift drag coefficient would be zero, and thus:

$$L_{duct} = \frac{1}{2}mv^2 = \frac{1}{2}pSlv^2 \tag{3.4}$$

$$W = \Delta KE = F\Delta x = Fl = L_{duct} \tag{3.5}$$

$$\frac{1}{2}pSlv^2 = Fl \tag{3.6}$$

$$L_{duct} = \frac{1}{2}\rho V^2 S C_{L_\alpha}\alpha \tag{3.7}$$

In which C_{L_α} is the duct lift coefficient; α_d is the angle between the inflow of wind and the duct, in which $\alpha_d = 90 - \alpha$; S is the propeller blade area.

4. Aerodynamic Resistance

Aerodynamic resistance in a ducted drone, like aerodynamic lift, is determinant on the air resistance for the fans (D_{duct}) and the air resistance for the drone's body (D_{CS}); thus:

$$D = D_{duct} \tag{3.8}$$

And D_{duct} is determined using the following equation:

$$D_{duct} = \frac{1}{2}\rho V^2 S(C_{D0d} + C_{D_\alpha d}\alpha) \tag{3.9}$$

In the equation, $C_{D_0 d}$ is the duct's zero-lift drag coefficient; $C_{D_\alpha d}$ is the drag coefficient under angle of attack (α).

5. Pitching Moment (Torque)

Aerodynamic force produces the pitching moment (torque) if it is applied at the aerodynamic center of the drone, but not at the center of pressure. Since the control rudder is eliminated from this drone, the pitching moment should only consist of that created by the duct, and thus:

$$M = F(l) = (L_{duct}sin(\alpha) + D_{Duct}cos(\alpha))(z_{C_m} - z_{C_p d}) \tag{3.10}$$

In which z_{C_m} and $z_{C_p d}$ is the center of mass's and the aerodynamic force's application point with respect to the center at O_{Z_b}.

If the drone is flying horizontally at a relative fast speed, then $cos(\alpha)$ and $sin(\alpha)$ would be negligible, and thus neglecting the air resistance, leaving the formula to:

$$M = L_{duct}(z_{C_m} - z_{C_p d}) \tag{3.11}$$

6. Side Force & Yawing Torque

For this drone the Side Force (Y) should consists of only the side force of the duct (Y_{duct}), and thus:

$$Y = Y_{duct} \tag{3.12}$$

And the equation of Y_{duct} should be the following:

$$Y_{duct} = \frac{1}{2}\rho V^2 S_d C_{Y_\beta d}\beta \tag{3.13}$$

With this being the formula for the force, the formula for Y_{yaw} torque should be:

$$N = (Y_{duct}cos(\beta) + D_{duct}sin(\beta))(z_{C_m} - Z_{C_p t}) \tag{3.14}$$

Because the Yaw angle (β) for high speed horizontal flying, $sin(\beta) \approx 0$ and $cos(\beta) = 1$, so the air resistance caused by the duct and control rudder could be neglected, making the equation:

$$N = Y_{duct}(Z_{C_m} - Z_{C_p t}) \tag{3.15}$$

7. Precession Torque

Due to the high spinning speed and the close-nit structure, when the drone is changing form, the fan would create a precession torque, allowing the pitch and the duct to create a strong coupling dynamic. With this, the precession torque could be expressed with:

$$M_{gyro} = \Omega \times J\omega \tag{3.16}$$

In which Ω is the propeller's angle of propelling vector; J is the vector for moment of inertia; ω is the drone's angle.

b. Forward Kinematics

This part analyze the forward kinematic part of the drone when it is attached to replicas of itself. This would help the drone to later calculate the position of all parts in the drone and could see how axis turns with each joint. The analysis would be based on three drones attached together as any more drones would follow the same shift logic. With forward Kinematics, the position and orientation of the end0effector could be determined by the joint variables.

1. Kinematic Chains

All joints in the robots have only one degree of freedom, so such would be assumed for all formulas in this part. This assumption won't lose generality since all joints could be thought as a succession to 1 DoF with links of length zero in between. With such an assumption, all the actions could be described by a single number: either the rotational angle in a revolute joint or the displacement in a prismatic joint. Any robot with *n* joints would have *n+1* joints and thus the numbering of joints would be from 1 to *n* and the number of links be from 0 to *n*. Since the location of joint *I* would be fixed with respect to link *i-1,* link *i* moves when joint *i* is actuated.

Since the i^{th} joint only has one degree of freedom, and in the case of the drone it could only be a revolute joint, there could be a joint variable associated with it denoted by q_i, making it $q_i = \theta_i$. Needing to perform kinematic analysis using this, a coordinate frame is attached to each joint. For example, the link *i* would have the coordinate frame of $o_i x_i y_i z_i$, so *i* would remain constant to its own coordinate frame however the joint *i* moved. Using this coordinate system, $o_0 x_0 y_0 z_0$ would be the inertial frame.

With this coordinating system, there could be a homogeneous transformation matrix (A_i) which expresses the position and orientation of $o_i x_i y_i z_i$ with respect to $o_{i-1} x_{i-1} y_{i-1} z_{i-1}$ (the coordinate frame of the link attached by the same link). With such, A_i would be a function of a single joint variable, in other words q_i, and thus: $A_i = A_i(q_i)$. Since there is only a theta change in this design, $A_i = A_i(\theta_i)$. Base transformation could then be denoted using a transformation matrix, denoted T_j^i. This matrix would express the position and orientation of $o_j x_j y_j z_j$ with respect to $o_i x_i y_i z_i$. This matrix would be a combination of all matrixes from A_i to A_j, and thus:

$$T_j^i = A_{i+1} A_{i+2} A_{i+3} \dots A_{j-2} A_{j-1} A_j \quad \text{if } i < j \tag{4.1}$$

$$T_j^i = I \quad \text{if } i = j \tag{4.2}$$

Since A_i is the base in this case, it should not be in the calculations, and *j* would always be larger than *i*.

T_j^i is the general formula for calculations, and when put into the context of this drone, the calculation would be done from 0 to the n^{th} frame (individual drone), which is denoted as matrix *H*. Matrix *H* would also, like *T* be a homogeneous transformation matrix, which is made of the component o_n^0 and R_n^0. o_n^0 is a three vector (3x1 matrix) that gives the coordination of the frame with respect to the origin. R_n^0 then is a 3x3 matrix that combines the rotational matrix of the three axis.

$$H = T_n^0 = \begin{bmatrix} R_n^0 & o_n^0 \\ 0 & 1 \end{bmatrix} \tag{4.3}$$

And combined with equation 3.1:

$$A_{i+1} \dots A_j = T_j^i = \begin{bmatrix} R_j^i & o_j^i \\ 0 & 1 \end{bmatrix} \tag{4.4}$$

From this, the form of A_i could be shown as

$$A_i = \begin{bmatrix} R_i^{i-1} & o_i^{i-1} \\ 0 & 1 \end{bmatrix} \tag{4.5}$$

And the form of R_j^i as

$$R_j^i = R_{i+1}^i R_{i+2}^{i+1} \dots R_{j-1}^{j-2} R_j^{j-1} \tag{4.6}$$

And o_j^i calculates as

$$o_j^i = o_{j-1}^i + R_{j-1}^i o_j^{j-1} \tag{4.7}$$

2. Denavit Hartenberg Convention

There are supposedly 6 variables in the calculations of position and orientation for the n^{th} frame; however, the calculation could be simplified to only 4 variables with the DH-Convention. After simplification, each A_i could be simplified into this equation:

$$A_i = Rot_{z,\theta_i} Trans_{z,d_i} Trans_{x,a_i} Rot_{x,\alpha_i} \tag{4.8}$$

$$= \begin{pmatrix} c_{\theta_i} & -s_{\theta_i} & 0 & 0 \\ s_{\theta_i} & c_{\theta_i} & 0 & 0 \\ 0 & 0 & 1 & 0 \\ 0 & 0 & 0 & 1 \end{pmatrix} \begin{pmatrix} 1 & 0 & 0 & 0 \\ 0 & 1 & 0 & 0 \\ 0 & 0 & 1 & d_i \\ 0 & 0 & 0 & 1 \end{pmatrix} \begin{pmatrix} 1 & 0 & 0 & a_i \\ 0 & 1 & 0 & 0 \\ 0 & 0 & 1 & 0 \\ 0 & 0 & 0 & 1 \end{pmatrix} \begin{pmatrix} 1 & 0 & 0 & 0 \\ 0 & c_{\theta_i} & -s_{\theta_i} & 0 \\ 0 & s_{\theta_i} & -c_{\theta_i} & 0 \\ 0 & 0 & 0 & 1 \end{pmatrix}$$

$$= \begin{pmatrix} c_{\theta_i} & -s_{\theta_i} c_{\alpha_i} & s_{\theta_i} s_{\alpha_i} & a_i c_{\theta_i} \\ s_{\theta_i} & c_{\theta_i} c_{\alpha_i} & -c_{\theta_i} s_{\alpha_i} & a_i s_{\theta_i} \\ 0 & s_{\alpha_i} & c_{\alpha_i} & d_i \\ 0 & 0 & 0 & 1 \end{pmatrix} \tag{4.9}$$

In this case, the four variables, rotational and transitional of both x and z would be enough for the calculation of a set frame. θ, d, α, and a are parameters associated with j and i, and $a_i, \alpha_i, d_i, \theta_i$ are link length, link twist, link offset, and joint angle respectively.

With the D-H convention, we could then calculate the $a_i, \alpha_i, d_i, \theta_i$ of each link in the system to be given below:

Link	a	α	d	θ
1	a_1	90	0	θ_1
2	0	90	d_2	θ_2
3	a_3	90	d_3	θ_3
4	0	90	0	θ_4
5	a_5	90	d_5	θ_5

V. Control

a. Kalman Filters

This projects uses the Kalman Filter to navigate the flight of the drone. It allows the drone to be measured from different sources of information, in this case gyroscope, ducted fan force, and IMU. The Kalman filter could combine all these measurements and provide the optimal estimate of where the drone is at a particular time. The following should be a mathematical approach to how Kalman filters are used in this project.

1. State Observers

The state observer will combine the actual measured results and the predicted results to estimate the system's true state. This part essentially adds the error between the predicted measurement and the actual measurement into the system in order to form a more accurate model. In this section e_r would be defined as error (to be distinguished from e), x as the measurement being predicted, y as the measurement which could be measured, u as the input value, and any variables with a hat would be the estimate state of the variable. Thus, we could include the first equations:

$$e_r = x - \hat{x} \tag{5.1}$$

The later parts would go into the actual mathematical model used to predict x and y, so for now, lets say the mathematical model is composed of the two following equations:

$$\dot{x} = Ax + Bu \tag{5.2}$$

$$y = Cx \tag{5.3}$$

And thus the equations of the estimated variables should be the following:

$$\dot{\hat{x}} = A\hat{x} + Bu + K(y - \hat{y}) \tag{5.4}$$

$$\hat{y} = C\hat{x} \tag{5.5}$$

By subtracting equations 5.4 from 5.2 and equation 5.5 from 5.3, there are the two following equations:

$$\dot{x} - \dot{\hat{x}} = Ax + Bu - (A\hat{x} + Bu + K(y - \hat{y})) \tag{5.6}$$

$$y - \hat{y} = C(x - \hat{x}) \tag{5.7}$$

Then substituting equation 5.1 and 5.7 into equation 5.6:

$$\dot{e}_r = (A - KC)e_r \tag{5.8}$$

Thus,

$$e_r(t) = e^{(A-KC)t}e_r(0) \tag{5.9}$$

From this we could conclude that if $(A - KC) < 1$, then $e_r(t) \to 0$ as $t \to \infty$, and KC give more control over the decaying speed of e_r rather than having it completely dependent on matrix A, which wouldn't always be exact due to the uncertainties in the mathematical model. Such would be the graphical representation of state observer:

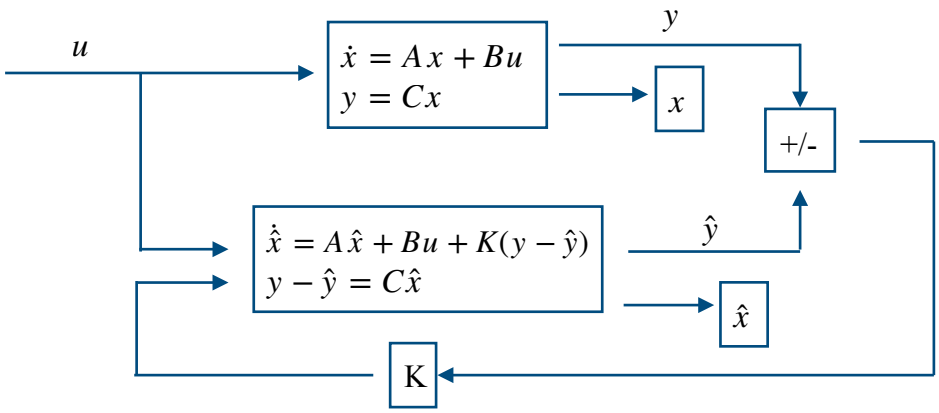

2. Noise Reduction Operator

In a real scenario, the equation, wouldn't be of simply equation 5.2 and 5.3, since there would be both measuring and processing noise represented as v and w respectively. Thus, the actual equation would be:

$$x_k = Ax_{x-1} + Bu_k + w_k \tag{5.10}$$

$$y_k = Cx_k + v_k \tag{5.11}$$

Although the noises won't follow a regular patter, it could be determined to be a Gaussian with a mean of 0 and a covariance of R:

$$v_k \sim N(0,R) \tag{5.12}$$
$$w_k \sim N(0,Q) \tag{5.13}$$

In which R is σ_v^2 and Q is σ_w^2. Since both are normal curves, simple multiplication could results in the best estimate for $\hat{x}_k$, and thus reducing the noise. Thus, by combining the measurement (y_k) and the predicted measurement ($\hat{x}_k$), the optimal estimate of $\hat{x}$ could be found. Graphically, it would be represented as the following:

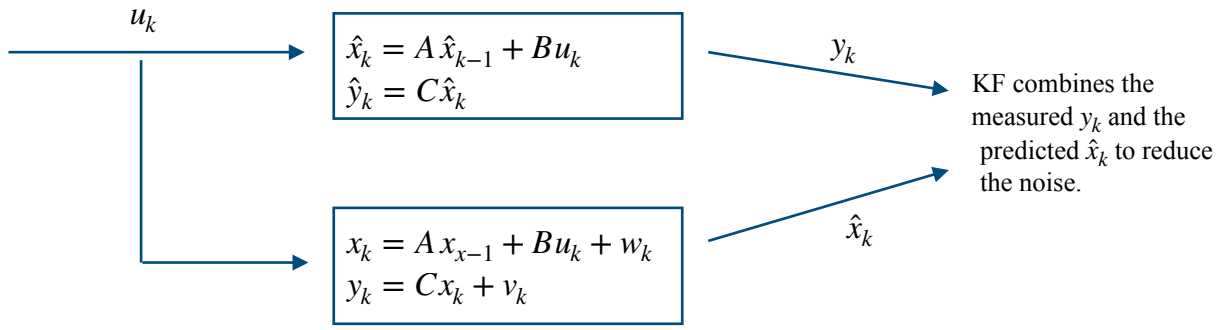

3. Combining State Observer and Noise Reduction Operator

In this section, the prior state estimate would be represented as $\hat{x}_k^p$ as to separate from the posteriori optimal estimate ($\hat{x}_k$). With this, the following equations are to predict the prior state estimate ($\hat{x}_k^p$) and the error covariance (P_k^p), which is the error variance for $\hat{x}_k^p$:

$$\hat{x}_k^p = A\hat{x}_{k-1} + Bu_k \tag{5.14}$$
$$P_k^p = AP_{k-1}A^T + Q \tag{5.15}$$

Then P_k^p and $\hat{x}_k^p$ are then updated to find the posteriori optimal estimate ($\hat{x}_k$) and the posteriori error covariance (P_k). To update, a variable K_k would have to be found, and it would determine the percentage of y_k and $\hat{x}_k^p$ used for updating $\hat{x}_k$, thus minimizing the posteriori error variance. The calculation of K_k, P_k, and $\hat{x}_k$ are listed below:

$$K_k = \frac{P_k^p C^T}{CP_k^p C^T + R} \tag{5.16}$$
$$P_k = (I - K_k C)P_k^p \tag{5.17}$$
$$\hat{x}_k = \hat{x}_k^p + K_k(y_k - C\hat{x}_k^p) \tag{5.18}$$

After P_k, and $\hat{x}_k$ are calculated by equation 5.17 and 5.18, they would become the new $\hat{x}_k^p$ and P_k^p. Then with new input, it would be in a constant loop between the updated and predicted.

b. PID (Proportional-Integral-Derivative Controller)

The mathematical model mentioned in Kalman Filter would be PID, a control calculation which help the drone remain its stable state. PID is the simple combination of control gain (K_p), integral time (K_i), and derivative time (K_d) in which the proportional is weighted as P, integral as P/K_i, and derivative as PK_d. To start with, the general formula for PID control is of the following:

$$u(t) = K_p e(t) + K_i \int_0^t e(t)dt + K_d \frac{d}{dt} e(t) \tag{6.1}$$

The first part of the equation, $K_p e(t)$, would add force to the fan opposite of the inclined direction. It would add it proportionally to the error, which is:

$$e(t) = 0° - \theta \tag{6.2}$$

Although this calculation could allow the drone to come back to balance, it would take a very long time. The drone would most likely be left in an oscillatory motion for a very long time.

In order to shorten the time for the drone to remain to its original state, the third part, $K_d \frac{d}{dt} e(t)$, is added to the equation. This part of the equation measures the change of error with respect to time and multiplies it by the derivative constant. This would allow the system to stabilize itself quickly in response to high error changes in a short period of time. However, this part of the system won't come into any use if the system isn't moving; in other words, if the drone somehow remains stable at an angle, it wouldn't move back to its original position. So, if the drone is constant at a small angle, neither the proportional part nor the derivative part would respond.

The second part of the equation, $K_i \int_0^t e(t)dt$, would help solve this problem; it helps the drone to remain horizontal. The integral value allows the small error values to add up and eventually making an effect on the fans. However, through testing, this part of the equation doesn't seem to help the stabilization of the drone since it has no demand to stay perfectly horizontal. Thus, through experiments, the three constant were decided as the following:

$$K_p = 2 \tag{6.3}$$

$$K_i = 0 \tag{6.4}$$

$$K_d - 0.2 \tag{6.5}$$

VI. Testing Results

a. Rotational Degree of Freedom Along X and Y Axis

The test is conducted to measure the maximum rotation along the x and y direction. This mainly tests the PMU6050's ability and its connection with the computer. The experimental procedures would be as follows:

1. Connect the computer with the main controller on the drone (esp32)
2. Control the servo's movement until it reaches maximum position along the x and y axis
3. Obtain data from the gyroscope on the drone and record the value after it's been transmitted to the computer
4. Analyze the data in the computer through graphing the change of angle to determine the maximum and minimum of rotation

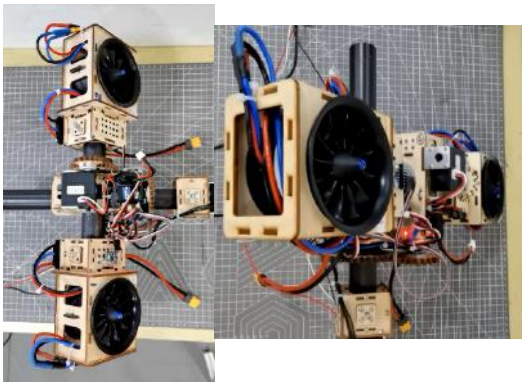

As shown in the picture, through control of the servos along the x and y axis, the ducted fan could achieve rotation with two degrees of freedom. MPU6050a, placed on the drone, could measure the rotational angle along the different axis and send it to the computer.

MATLAB is ten used to create the analysis of these signals, and it produced analysis as follows:

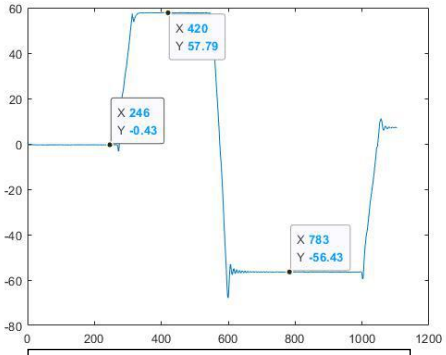

Figure 6.1: Rotational Angle along x-axis

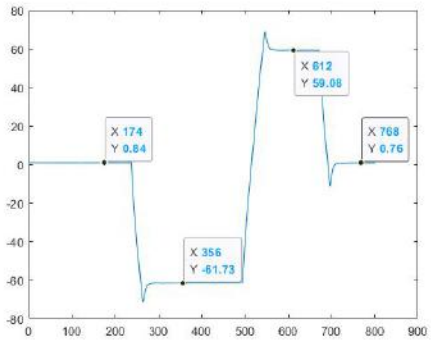

Figure 6.2: Rotational Angle along y-axis

With such we would know the maximum rotation angle to be as the following table:

Axis of Rotation	Direction	Maximum Angle	Change in Angle
x-axis	Forward	59.08°	120.73°
	Backward	-61.73°	
y-axis	Forward	57.79°	114.22°
	Backward	-56.43°	

Such angle of rotation would be enough for the drone to reach flexibility in air.

b. Ducted Fan Lift Test

This experiment tries to determine the relationship between PWM values and thrust. This is determined using the drone, the computer, and an electric weight, with the following procedures:

1. Record the original weight of the drone
2. Make the drone increase its PWM value (from 1000 to 2000), record the data
3. Repeat process 2 until the drone takes flight
4. Analyze the PMW value's relationship with weight

Data Recorded

PWM	Wieght	PWM	Weight	PWM	Weight
1000	1463.9	1160	1067.3	1320	606.3
1020	1463.9	1180	997.8	1340	506.3
1040	1463.9	1200	942.7	1360	465.8
1060	1362.9	1220	873.3	1380	443.5
1080	1245.3	1240	812.3	1400	390.6
1100	1300.15	1260	766.8	1420	316.5
1120	1245.3	1280	706.3	1440	287.2
1140	1183.6	1300	648.7	1460	246.5

Analysis:

Using MATLAB, the following graph had been drawn:

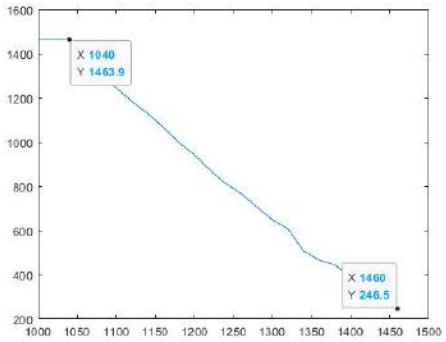

Figure 6.3: Relationship between PWM value and weight of drone

From the graph, we could see the linear relationship between the two and thus we could use determine the relationship as the two. When PWM value reaches 1060, the ducted fan would start and the linear relationship would be described as:

$$F=-2.888(PWM)+4417$$

$$F=mg-F_{lift}$$

In which F is the difference between gravity and lift, PWM as the duty ration, mg as the weight of the drone, and F_{lift} as the lift. When F> 0, gravity would be greater than lift, making the drone unable to fly; when F=0, the gravity and lift would be equal, achieving hovering; when F<0, the lift would be greater than gravity, allowing for flight.

VII. Future Application

Currently, the drone had reached the state of hovering either by itself or with another drone attached. It could also transform in shape with respect to another drone. Due to the limitations of time, the drone haven't been able to recognize objects and transform its shape with regard to the object. However, the drone has all the function to do so, and those function had been tested. The practicability of the idea had also been tested and calculated through forward kinematics and force analysis. With more time, this drone, luckily, would be able to achieve all the intentions which I had for it, and the process with this project would not stop until its goals are reached. With such a drone, like microbots, it would be able to perform multiple functions of drones all in one, since it would be able to transform itself and perform at different needs.

IX. References

1. Falanga, D. , Mueggler, E. , Faessler, M. , & Scaramuzza, D. . (2017). Aggressive Quadrotor Flight through Narrow Gaps with Onboard Sensing and Computing using Active Vision. Proceedings - IEEE International Conference on Robotics and Automation. IEEE.
2. Hintz, C., Torno, C., & Carrillo, L. R. G. (2014, May). Design and dynamic modeling of a rotary wing aircraft with morphing capabilities. In *2014 International Conference on Unmanned Aircraft Systems (ICUAS)* (pp. 492-498). IEEE.
3. Zhao, M., Anzai, T., Okada, K., Kawasaki, K., & Inaba, M. (2021). Singularity-Free Aerial Deformation by Two-Dimensional Multilinked Aerial Robot With 1-DoF Vectorable Propeller. *IEEE Robotics and Automation Letters* , *6* (2), 1367-1374.
4. Jothiraj, W., Miles, C., Bulka, E., Sharf, I., & Nahon, M. (2019, June). Enabling bidirectional thrust for aggressive and inverted quadrotor flight. In *2019 International Conference on Unmanned Aircraft Systems (ICUAS)* (pp. 534-541). IEEE.
5. Nemati, A. (2016). *Designing, modeling and control of a tilting rotor quadcopter* (Doctoral dissertation, University of Cincinnati).
6. Zhao, M., Shi, F., Anzai, T., Okada, K., & Inaba, M. (2020). Online motion planning for deforming maneuvering and manipulation by multilinked aerial robot based on differential kinematics. *IEEE Robotics and Automation Letters* , *5* (2), 1602-1609.
7. Endo, G., Hagiwara, T., Nakamura, Y., Nabae, H., & Suzumori, K. (2018, July). A proposal of super long reach articulated manipulator with gravity compensation using thrusters. In *2018 IEEE/ASME International Conference on Advanced Intelligent Mechatronics (AIM)* (pp. 1414-1419). IEEE.
8. Saldana, D., Gabrich, B., Li, G., Yim, M., & Kumar, V. (2018, May). Modquad: The flying modular structure that self-assembles in midair. In *2018 IEEE International Conference on Robotics and Automation (ICRA)* (pp. 691-698). IEEE.
9. Kumar, R., Deshpande, A. M., Wells, J. Z., & Kumar, M. (2020, April). Flight control of sliding arm quadcopter with dynamic structural parameters. In *2020 IEEE/RSJ International Conference on Intelligent Robots and Systems (IROS)* (pp. 1358-1363). IEEE.
10. Anzai, T., Zhao, M., Nozawa, S., Shi, F., Okada, K., & Inaba, M. (2018, May). Aerial grasping based on shape adaptive transformation by halo: Horizontal plane transformable aerial robot with closed-loop multilinks structure. In *2018 IEEE International Conference on Robotics and Automation (ICRA)* (pp. 6990-6996). IEEE.
11. Oosedo, A., Abiko, S., Narasaki, S., Kuno, A., Konno, A., & Uchiyama, M. (2015, May). Flight control systems of a quad tilt rotor unmanned aerial vehicle for a large attitude change. In *2015 IEEE International Conference on Robotics and Automation (ICRA)* (pp. 2326-2331). IEEE.
12. Shi, F., Zhao, M., Anzai, T., Chen, X., Okada, K., & Inaba, M. (2019, May). External wrench estimation for multilink aerial robot by center of mass estimator based on distributed imu system. In *2019 International Conference on Robotics and Automation (ICRA)* (pp. 1891-1897). IEEE.
13. Gabrich, B., Saldana, D., Kumar, V., & Yim, M. (2018, May). A flying gripper based on cuboid modular robots. In *2018 IEEE International Conference on Robotics and Automation (ICRA)* (pp. 7024-7030). IEEE.
14. Falanga, D., Kleber, K., Mintchev, S., Floreano, D., & Scaramuzza, D. (2018). The foldable drone: A morphing quadrotor that can squeeze and fly. *IEEE Robotics and Automation Letters* , *4* (2), 209-216.
15. Zhao, M., Kawasaki, K., Chen, X., Noda, S., Okada, K., & Inaba, M. (2017, May). Whole-body aerial manipulation by transformable multirotor with two-dimensional multilinks. In *2017 IEEE International Conference on Robotics and Automation (ICRA)* (pp. 5175-5182). IEEE.
16. Zhao, M., Shi, F., Anzai, T., Chaudhary, K., Chen, X., Okada, K., & Inaba, M. (2018, October). Flight motion of passing through small opening by dragon: Transformable multilinked aerial robot. In *2018 IEEE/RSJ International Conference on Intelligent Robots and Systems (IROS)* (pp. 4735-4742). IEEE.
17. Park, S., Lee, Y., Heo, J., & Lee, D. (2019, May). Pose and posture estimation of aerial skeleton systems for outdoor flying. In *2019 International Conference on Robotics and Automation (ICRA)* (pp. 704-710). IEEE.
18. Yang, H., & Lee, D. (2015, May). Hierarchical cooperative control framework of multiple quadrotor-manipulator systems. In *2015 ieee international conference on robotics and automation (ICRA)* (pp. 4656-4662). IEEE.
19. Sakaguchi, A., Takimoto, T., & Ushio, T. (2019, June). A novel quadcopter with a tilting frame using parallel link mechanism. In *2019 International Conference on Unmanned Aircraft Systems (ICUAS)* (pp. 674-683). IEEE.
20. Williams, C., & Hall, D. (Directors). (2014). *Big Hero 6* [Film]. Walt Disney Studios Motion Pictures
21. Williams, C., & Hall, D. (Directors). (2014). *Big Hero 6* [Film]. Walt Disney Studios Motion Pictures
22. Brewster, S. (2021, December 31). The Best Drones for Photos and Video. New York Times. https://www.nytimes.com/wirecutter/reviews/best-drones/